INTERNATIONAL SOCIETY FOR SOIL MECHANICS AND GEOTECHNICAL ENGINEERING

The paper was published in the proceedings of the 10th International Conference on Physical Modelling in Geotechnics and was edited by Moonkyung Chung, Sung-Ryul Kim, Nam-Ryong Kim, Tae-Hyuk Kwon, Heon-Joon Park, Seong-Bae Jo and Jae-Hyun Kim. The conference was held in Daejeon, South Korea from September 19th to September 23rd 2022.

Physical Modelling in Geotechnics
© 2022 KOREAN GEOTECHNICAL SOCIETY (KGS), Seoul, Korea, ISBN 978-89-952197-7-5

Centrifuge tests on foundations under alternating loads in overconsolidated clay

A. Ganal & O. Reul
Department of Geotechnical Engineering, University of Kassel, Germany

S.W. Jacobsz
Department of Civil Engineering, University of Pretoria, South Africa

ABSTRACT: To investigate the time-dependent load-deformation behaviour of foundations under alternating loads in overconsolidated clay, centrifuge tests on rafts and piled rafts in Kaolin clay are carried out. The foundations are subjected to unloading and reloading processes as well as to groundwater lowering, simulating typical loading scenarios of structures in an urban environment. In the scope of this paper initial results are presented and are discussed in the light of previous research on the distribution of pile resistances within piled rafts and the influence of the consolidation process.

Keywords: Centrifuge modelling, overconsolidated clay, piled raft, consolidation, pile resistances

1 INTRODUCTION

The prediction of the time-dependent load-settlement behaviour of foundations in clayey soils is particularly important when existing and new foundation elements are to be integrated, which is becoming increasingly important, especially in inner-city areas (Butcher et al. 2006). In order to be able to exploit further optimization potential by coupling existing foundations with new buildings, the time-dependent deformation behaviour of foundations caused by both consolidation processes and the time-dependent material behaviour (creep) of soils must therefore also be taken into account.

In addition to the time-dependent deformation behaviour of the soil and variable building loads resulting from demolition and reconstruction phases, construction activities in the surrounding area also influence the long-term deformation behaviour of foundations. In particular, the influence of neighbouring groundwater drawdowns has to be considered in this context, resulting in alternating stresses due to changes in the uplift and the effective stresses in the subsoil.

To investigate these topics, centrifuge tests on rafts and piled rafts in overconsolidated Kaolin clay were carried out. Further research activities in terms of this project include the evaluation and back-analysis of available long-term field measurements on high-rise buildings in Frankfurt Clay (Franzen & Reul 2022).

This paper presents the results of the first centrifuge test on a piled raft which was intended to enable optimization of the remaining investigation program.

2 CENTRIFUGE TEST

2.1 General remarks

The centrifuge test described below has been carried out in the beam centrifuge at the University of Pretoria with a platform radius of 3m capable of spinning up to 1500 kg to an acceleration of 100g (Jacobsz et al. 2014).

The test program comprised centrifuge tests on vertically loaded piled rafts and raft foundations under alternating vertical loads and varying ground water (gw) level, respectively. This paper focuses on the first test carried out on a piled raft with a constant gw level, while the results achieved for other configurations will be the subject of future publications.

All tests have been executed at a nominal centrifugal acceleration of 80g. The results presented throughout the paper are at model scale.

2.2 Experimental setup

The general test layout is shown in Fig. 1 in a cross section and a ground plan. The raft, a square, 150 mm × 150 mm aluminium plate (thickness t_r =16 mm) was placed in a strong box with a ground area of 400 mm × 600 mm. Applying the definition by Horikoshi & Randolph (1997) the raft-soil stiffness ratio can be established to $K_{rs} \approx 100$ indicating an essentially rigid raft. Beneath the raft 16 piles were installed in a 4 × 4 grid (spacing of $e = 4d_p$). The model piles comprised smooth aluminium tubes (wall thickness t_p = 1.25 mm) with a diameter of d_p = 10 mm and a length of L_p = 150 mm. The pile heads fitted into recesses in the raft resulting in a rigid connection in horizontal direction.

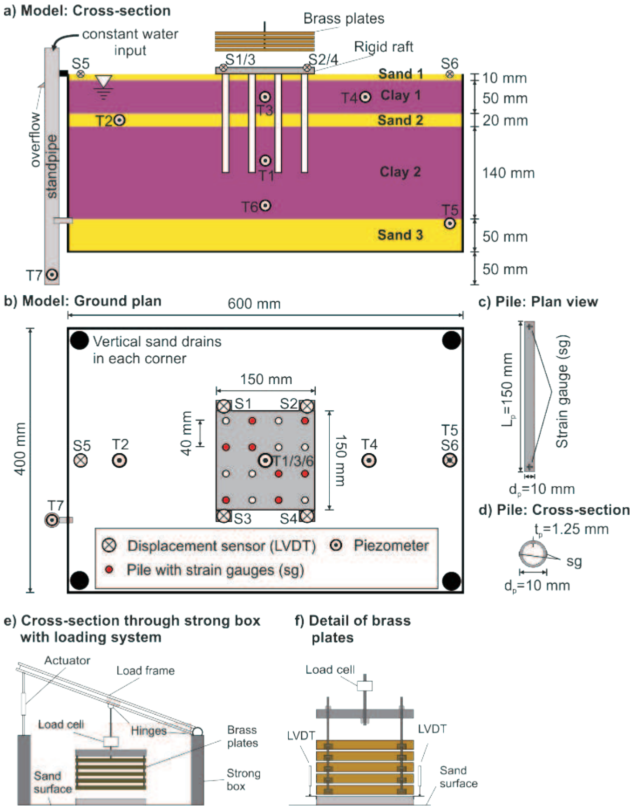

Fig. 1. Test layout.

To apply the load, five brass plates were lowered separately onto the raft with the help of a linear actuator (Fig. 1e, f). To monitor the load actually applied to the raft, the weight of the brass plates carried by the load frame was measured by a load cell, i.e. the load P applied on the raft is the difference between the weight of all brass plates and the force measured by the load cell.

The soil stratigraphy in the centrifuge tests comprised 10 mm of sand (Sand 1) to ensure a proper contact between raft and soil, followed by 50 mm of overconsolidated clay (Clay 1), 20 mm of sand (Sand 1) and overconsolidated clay (Clay 2) extending to a depth of 220 mm. A 50 mm thick sand layer (Sand 3) at the base of the strong box, separated from Clay 2 by means of a thin geotextile, served as a drainage layer. The water table was kept constant at 20 mm below ground level.

The instrumentation in the tests included four piezometers in Clay 1 and Clay 2 to monitor the consolidation process and three piezometers located in Sand 2, Sand 3 and in the standpipe used to control the groundwater level. It should be noted that the indicated piezometer depths may differ from the final position, as they have been installed into the slurry clay.

The vertical displacements of the raft were measured by means of four LVDT displacement transducers. Another two displacement transducers were used to measure the surface displacements.

Eight piles were equipped with one pair of strain gauges at the pile head and one pair of strain gauges at the pile base to derive the axial load transferred to the piles using the mean axial strain ε_a and the cross sectional stiffness EA (Fig. 1c, d). In the scope of this paper, pile loads at the pile head and pile base are termed pile resistance R and pile base resistance R_b, respectively. The pile shaft resistance R_s can be calculated as the difference between pile resistance and pile base resistance. The piles equipped with strain gauges were chosen so that at least two piles of each position (corner, edge, centre) have been instrumented (Fig. 1b).

2.3 Model preparation

In the preparation of the model, a drainage layer of sand was placed at the base of the box with a thin geotextile on top. Clay layer 2 was consolidated from a Kaolin slurry with a water content of 100 %, initially using weights gradually applied to 12 kPa. To produce an overconsolidated sample, a stress of $p = 246$ kPa was subsequently applied in several steps to the surface using a hydraulic press. During the consolidation, both the pore pressure and the settlement of the sample were monitored. The load was increased once the excess pore pressure had dissipated and the settlements completed. After the consolidation process monitored by means of piezometers was completed, Sand 2 was rained at an estimated dry density of $\rho_d = 1700$ kg/m^3. The procedure was then repeated for layers Clay 1 and Sand 1. The overconsolidation OCR ratio profile from this temporary loading is shown in Fig. 2a for a model at 80g.

To ensure internal equalisation of water heads in the different soil layers, vertical sand drains were installed in the four corners of the box.

2.4 Soil properties

The strength characterisation of the sample was undertaken immediately after the centrifuge test by means of a cone penetrometer (Fig. 2b). The penetrometer test was carried out at 80g after a short stop of the centrifuge to remove the actuator. Assuming a correction factor of $N_{kt} = 15$ the undrained shear strength averages approximately $s_u \approx 29$ kPa for Clay 1 (below gw) and $s_u \approx 74$ kPa for Clay 2, respectively.

The properties of the Kaolin clay used to prepare the clay layers are listed in Table 1. The properties of the sand are summarized in Table 2.

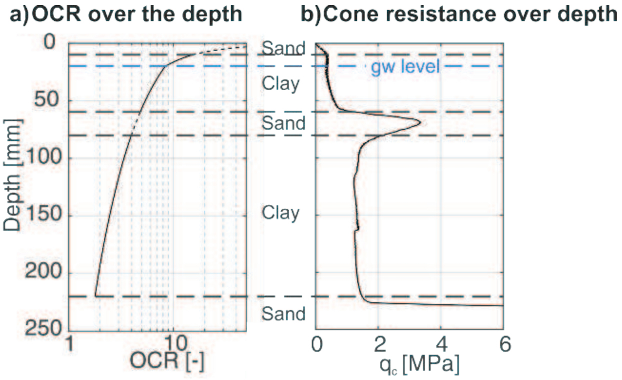

Fig. 2. Soil profile.

Table 1. Properties of the Kaolin clay.

Parameter			
Saturated unit weight	γ_{sat}	[kN/m³]	16.6
Plastic limit	PL	[%]	36
Liquid limit	LL	[%]	47
Percentage of particles d < 0.002 mm	-	[%]	31
Activity	I_A	[-]	0.35
Critical friction angle	φ_c	[°]	27
Compression index	C_c	[-]	0.129
Swelling index	C_s	[-]	0.030
Viscosity index	I_v	[-]	0.01

Table 2. Properties of the sand.

Parameter			
Mean grain size (mm)	d_{50}	[mm]	0.283
Effective grain size (mm)	d_{10}	[mm]	0.138
Critical friction angle (°)	φ_c	[°]	33
Coefficient of uniformity	C_U	[-]	2.32

2.5 Testing procedure

After the sample had been completed, the piled raft was jacked into the soil as a group at 1g using a press. It is assumed that the behaviour of 'pre-jacked' piles is comparable to bored piles in the field (Li et al. 2010).

Water was only added to the model shortly before starting the centrifuge to prevent excessive swelling of the Kaolin. The water was added to the model via a standpipe connected to the strong box. To keep the gw level constant throughout the test, water was added continuously to the standpipe, with an overflow ensuring the desired height.

In the test presented in this paper the gw level was held constant while the foundation was loaded by means of the brass plates lowered subsequently onto the raft. The loading scheme included a temporary unloading and reloading sequence and two consolidation phases where the load was held constant over a longer time period as summarized in Table 3.

3 RESULTS

3.1 General remarks

Before starting the loading sequence, the sample was allowed to consolidate under its weight with the development of settlements and the dissipation of excess process monitored. During this process, the centrifuge had to be stopped and restarted twice unscheduled which is believed to have increased the settlements of the foundation significantly. In the remainder of this paper, all results presented refer to the start of the main loading sequence, i.e. to the end of the consolidation process.

Fig. 3 shows the development of the load on the foundation due to the plates successively lowered onto the raft. In the first two loading phases the load decreased shortly after the lowering of the respective brass plates due to problems in the load application. From loading phase 3 on the brass plates had been adjusted to achieve a correct load transfer to the raft. During the loading in phase 8, the full weight of a fifth brass plate could not be fully applied.

Table 3. Loading scheme.

Phase		Time t [min]	Load p [kPa]
1	loading	20.5	65
2	loading	20.5	115
3	loading	20.5	185
4	loading	20.5	250
5	consolidation	328.5	250
6	unloading	20.5	185
7	reloading	20.5	250
8	loading	20.5	275
9	consolidation/creep	821.2	275

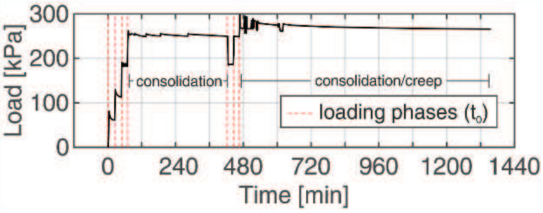

Fig. 3. Variation of load with time.

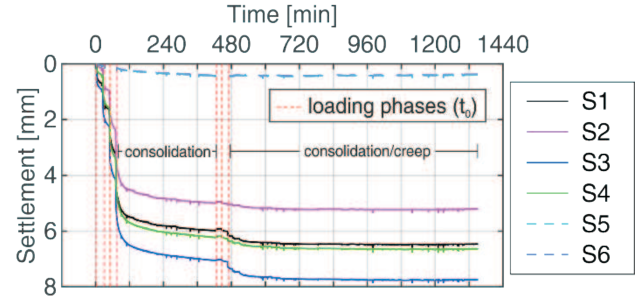

Fig. 4. Variation of settlements with time.

3.2 Settlements

The variation of settlements with time is plotted in Fig. 4 for all six displacement transducers. While the sensors S5 and S6 located on the soil surface show more or less identical settlements, the other sensors placed on the raft indicate relatively large differential settlements which might have been caused by the load plates not being lowered exactly vertically.

Although the load increments amount to $\Delta p = 68$ kPa in each loading phase, the increase in settlement became significantly larger as the load increased. This may be due to the overconsolidation ratio of the soil approaching OCR = 1 during the loading process. It is also interesting to note that during the unloading phase only a small amount of heave of the raft can be observed.

3.3 Pore pressures

Fig. 5 shows the variation of pore pressures with time for the piezometers T2, T5 and T7 in the sand and the standpipe, respectively, and piezometers T1 and T6 in Clay 2. T3 and T4 in Clay 1 proved not functional.

The decrease of pore pressure at T5 and T7, which shows the hydrostatic water pressure at their respective depths, was caused by an inadequate water supply to the standpipe which was fixed after 480 min, resulting in an illustrated increase in pore pressure.

The several loading phases applied is evident from the buildup of excess pore pressures in the clay (T1, T6).

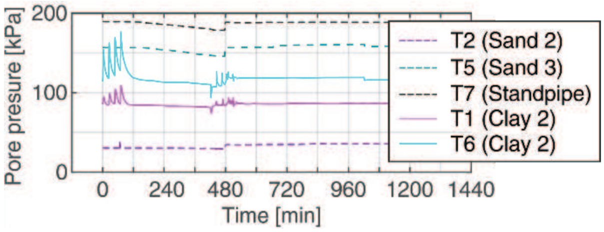

Fig. 5. Variation of pore pressure with time.

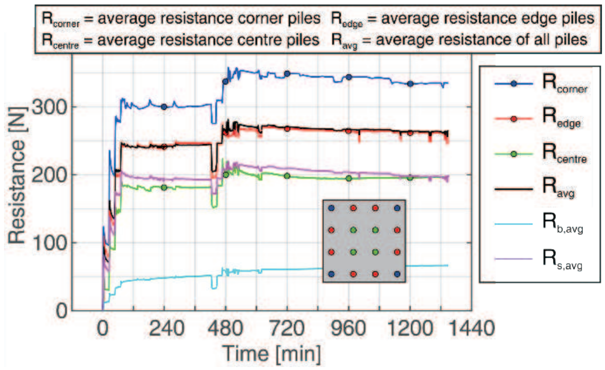

Fig. 6. Variation of pile resistances with time.

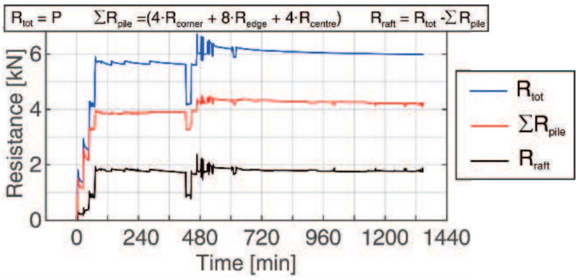

Fig. 7. Variation of total resistance, raft resistance and sum of all pile resistances with time.

3.4 Pile resistances

In-situ measurements (e.g. Sommer et al. 1985) and numerical simulations (e.g. Reul 2004) indicate that the pile resistance, i.e. the pile head load, of a pile in a piled raft strongly depends on the position of this pile in the pile group. Under working load conditions the pile resistance can be expected to increase from centre piles to edge piles to corner piles which is confirmed in Fig. 6 by the results of the centrifuge tests. Fig. 6 also separates the weighted average pile resistance R_{avg} into the contribution of the pile shaft resistance $R_{s,avg}$ and the pile base resistance $R_{b,avg}$. As can be expected for piles in a relatively homogenous soil, the shaft resistance is responsible for the major share of the pile resistance, amounting to 81% in phase 1 and 79 % in phase 4.

The variation of total resistance, raft resistance and sum of all pile resistances ΣR_{pile} with time is documented in Fig. 7. For this plot, the raft resistance R_{raft} was calculated as the difference between the total resistance R_{tot}, which is equal to the measured load applied on the foundation (i.e. the dead weight of the raft not taken into account), and the sum of all pile resistances ΣR_{pile} which has been calculated from the weighted average of the measured pile resistances.

The load share between piles and raft is quantified by the piled raft coefficient α_{pr}:

$$\alpha_{pr} = \frac{\Sigma R_{pile}}{R_{tot}} \tag{1}$$

The measurements confirm previous findings (e.g. Reul 2004) that the load share between piles and raft is not constant for a certain piled raft configuration, but generally decreases with increasing load level. During the centrifuge test the piled raft coefficient decreased from $\alpha_{pr} = 0.83$ (phase 1) to $\alpha_{pr} = 0.69$ (phase 4). It is interesting to note that during a loading phase, i.e. after the load had been applied and held constant for a period of time, the piled raft coefficient increased. For example, in phase 4, the piled raft coefficient increased from $\alpha_{pr} = 0.67$ immediately after the load had been applied within approximately 20 min to the value of $\alpha_{pr} = 0.69$ mentioned above. This phenomenon is a result of the consolidation process as predicted based on numerical simulations (Reul 2002).

4 CONCLUSIONS

The centrifuge test data presented in the scope of this paper shows good agreement with previous research on the distribution of pile resistances within piled rafts and the influence of the consolidation process on the bearing behaviour of piled rafts. In addition, valuable information was obtained for process improvement for further tests planned within the scope of this research project. Future tests will especially focus on the effect of unloading-reloading sequences and also investigate the influence of changes in the groundwater level.

ACKNOWLEDGEMENTS

The overall project is funded by the Deutsche Forschungsgemeinschaft (DFG, German Research Foundation) - RE 3881/4-1.

REFERENCES

Butcher A.P., Powell J.J.M. & Skinner H.D. 2006. Reuse of foundations for urban sites. *IHS BRE Press, Bracknell.*

Franzen A. & Reul O. 2022. Numerical investigation of the long-term settlement behaviour of piled rafts in over-consolidated clay. *Proc. 20th ICSMGE, Sydney* (accepted for publication)

Horikoshi K. & Randolph M.F. 1997. On the definition of raft-soil stiffness ratio. *Géotechnique 47, 5, 1055–1061*

Jacobsz S.W., Kearsley E. & Kock J.H.L. 2014. The geotechnical centrifuge facility at the University of Pretoria. *Proc. 8th Int. Conf. on Physical Modelling in Geotechnics*, 169-174

Li Z., Haigh S.K. & Bolton M.D. 2010. The response of pile groups under cyclic lateral loads. *Int. Journal of Physical Modelling in Geotechnics 10: 47–57.*

Reul, O. 2002. Study of the influence of the consolidation process on the calculated bearing behaviour of a piled raft. *Proc. 5th NUMGE, Paris,* 383-388

Reul, O. 2004. Numerical study of the bearing behaviour of piled rafts. *Int. Journal of Geomechanics, Vol. 4, Issue 2,* 59-68

Sommer, H., Wittmann, P. & Ripper, P. 1985. Piled raft foundation of a tall building in Frankfurt clay. *Proc. 11th ICSMFE, San Francisco, 4,* 2253–2257